Subdivision and G-spline hybrid constructions for high-quality geometric and analysis-suitable surfaces

Jörg Peters[1] and Kęstutis Karčiauskas[2]

[1] University of Florida, USA,
jorg.peters@gmail.com,
WWW home page: https://www.cise.ufl.edu/∼jorg/
[2] Vilnius University, Lithuania

Abstract. This survey of piecewise polynomial surface constructions for filling multi-sided holes in a smooth spline complex focusses on a class of hybrid constructions that, while heterogeneous, combines all the practical advantages of state-of-the-art for modelling and analysis: good shape, easy implementation and simple refinability up a pre-defined level.
After reviewing the three ingredients – subdivision, G-spline and guided surfaces – the hybrid is defined to consist essentially of one macro-patch for each of n sectors, leaving just a tiny n-sided central hole to be filled by a G-spline construction. Here tiny means both geometrically small, e.g. two orders of magnitude smaller than pieces of the spline complex, and small in its contribution to engineering analysis, i.e. it is unlikely to require further refinement to express additional geometric detail or resolve a function on the surface, such as the solution of a partial differential equation.
Each macro-patch has the local structure of a subdivision surface near, but excluding the central, extraordinary point: all internal transitions are the identity or scale according to contraction speed toward the extraordinary point. Both the number of pieces of the macro-patches and the speed can be chosen application-dependent and adaptively.

Keywords: free-form spline surface, subdivision surface, G-spline, guided surface, accelerated subdivision, refinability

1 Introduction

A hybrid construction for filling an n-sided hole in a spline complex consists of two parts: a main body formed by several nested surface rings and a tiny central n-sided cap, see Fig. 1, b,h. Each ring consists of n L-shaped sectors that fit together smoothly at their tips to form a curved annulus, called surface ring. The L-shape also joins smoothly with a smaller L-shaped sector of the next ring, as illustrated in Fig. 2. The surface rings form a nested sequence that contracts rapidly towards the center. Alternatively, one can think of each L-shape as a 4-sided macro-patch with one quadrant punched out to leave space for the next smaller L-shape, i.e. their union is a spline complex with a hole. This is the setup of subdivision algorithms [82] near extraordinary points, except that the process in the hybrid construction stops after a few steps, e.g. 2 or 3 nested surface rings.

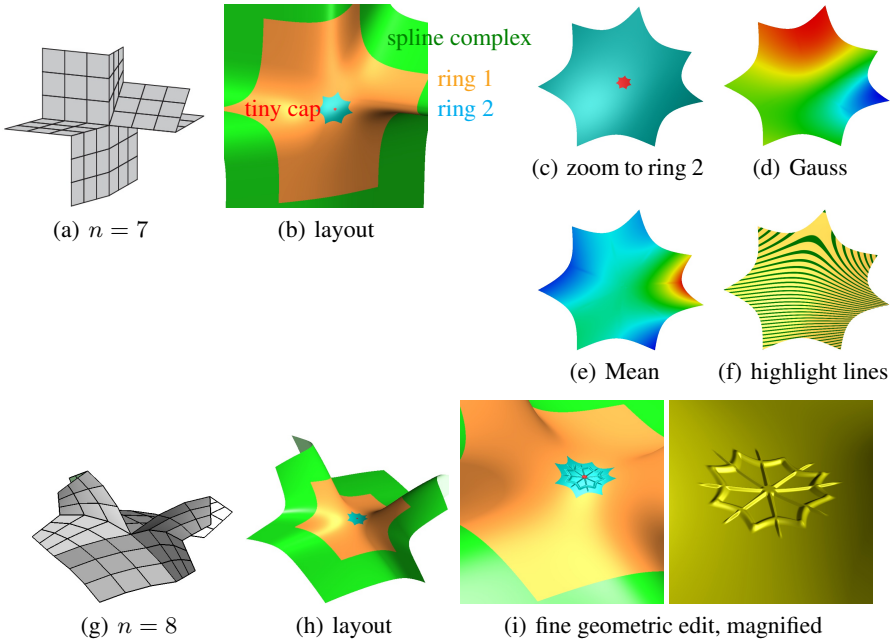

Fig. 1. Examples of high-valence hybrid surfaces. (a,g) Generalized control net (**c**-net). (b,h) layout of surface rings with almost invisible tiny cap. (c–f) Shape interrogation of ring 2 and the tiny cap: (d) Gauss curvature, (e) mean curvature. (i) Localized degrees of freedom used to emboss a pattern [46].

The pieces join to form the main body of the surface without change of variables, except possibly scaled derivatives as we adjust the contraction 'speed' of the rings. The main body of the surface is therefore amenable to refinement by knot insertion to increase of degrees of freedom. The same holds for functions on the surface, such as textures.

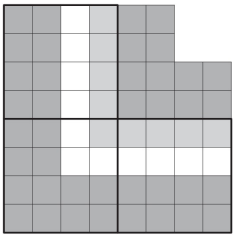

Fig. 2. L-shaped sectors forming a macro-patch (fine lines form a bi-quartic (bi-4) BB-net [20].

Only the tiny central n-sided cap is assembled by joining pieces so that derivatives agree after a change of variables (reparameterization), i.e. the cap is G^k continuous. The cap can be one of many in the literature, see Section 4. Typically the cap is so small that it needs not be refined. If it needs to be refined, [55] provides a refinable G^2 tiny cap construction.

The hybrid structure seems to just delay the multi-sided hole-filling challenge. The motivation for this seemingly more complex approach is that, if the cap is chosen to be smaller than the maximally anticipated refinement – for geometric modeling or computing on surfaces – then all surface pieces share a simple parameterization for refinement. On the other hand, capping the rings avoids the infinite recursion and central singularity of subdivision surfaces that necessitate smart data structures and special algorithms for proper

integration over infinitely many polynomial pieces. By construction a hybrid surface is therefore 'analysis-suitable', in the sense that it offers a uniform increase in degrees of freedom by knot insertion – up to the refinement level of the tiny cap (and further, at some cost in complexity, if the cap is chosen to be refinable).

To ensure that the hybrid constructions are 'geometry-suitable', i.e. yield good shape, a third technique is applied: both the main body and the cap follow a guide surface. A guide surface need not match the surrounding spline complex but is sampled ever closer to the central point to guarantee that subsequent rings and the tiny cap do not freely oscillate but follow a consistent, structurally simpler shape.

Overview. Section 2 classifies constructions for filling n-sided holes and explains requirements for geometric design and engineering analysis. Section 3 reviews subdivision algorithms, Section 4 reviews G-splines, and Section 5 reviews guided constructions, the three ingredients from which subdivision-and-G-spline-hybrids are built in Section 6.

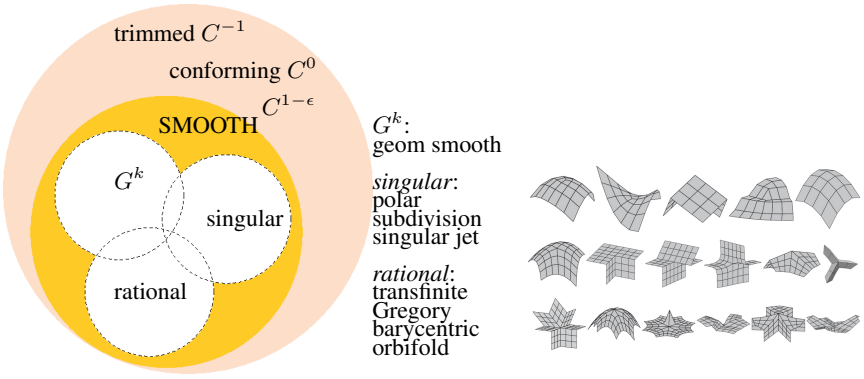

(a) Classification of constructions (b) quad-net obstacle course

Fig. 3. (a) Categories of surface parameterizations for irregular configurations from [80]. (b) Examples of meshes in the quad-net obstacle course [37] that serve as test control nets for the geometric suitability of constructions analogous to the finite element obstacle course for engineering analysis.

2 Categories of and requirements for surfaces with irregular configurations

Fig. 3(a) proposes a partition of the universe of spline constructions for irregular configurations. The main irregular configurations are illustrated in Fig. 4: star-configurations, multi-sided facets, T-junctions and polar configurations. The partition groups by smoothness, polynomiality and singularity of the surface parameterization. The topmost entry, *trimmed NURBS* surfaces, is the de facto industry standard. Trimming means restricting the domain of surface pieces by curves in the domain. In styling software, polynomial

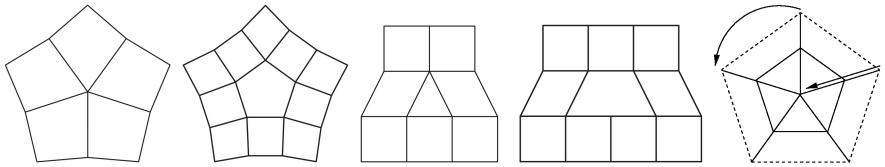

(a) star-net (b) n-gon-net (c) τ_0-net (d) τ_1-net (e) polar-net

Fig. 4. Locally quad-dominant mesh patterns (see [54]). The valence in (a,b,e) is $n = 5$. The pentagon in (d) is a T_1-gon, the triangle in (c) is a T_0-gon.

pieces are typically laid down to capture primary shape, cut back where they overlap and blended by fillet transition surfaces. This approach preserves simple, elegant shape in the large but ultimately forces stylists to devote ever more time to ever smaller blends between the primary surfaces [105].

Conforming C^0 surfaces, including curved triangulations, are ubiquitous and sufficient for basic engineering analysis (volume, homogeneous material moments, linear elasticity, etc.) and in computer graphics, where visual appearance trumps accurate geometry, [101, 64, 28]. Generalized barycentric patches, e.g. [65, 94], and non-4-sided transfinite constructions, e.g. [15, 86, 99, 100, 88], cover multi-sided holes with single, typically C^∞ patches. Due to an underlying very high rational degree, exactly computing their higher-order derivatives is costly. Due to its focus on free-form surfaces, the classification leaves out analysis-suitable functions and their graphs, e.g. [95, 33]. Subdivision surfaces and G^k constructions will be discussed individually in the Section 3 and Section 4.

2.1 Requirements on the geometry

The quality of a surface is a subjective term. Two tools are commonly used to assess geometric quality: 'curvature profiles' superimpose the curvature function of planar cuts orthogonal to the surface (Fig. 1d,e show the less common shading of the whole surface by Gauss and Mean curvature); and 'highlight lines' [6] approximate the effect of parallel arrangement of tube lights in a car show room. Unless explicitly intended as a surface feature, artifacts such as abrupt changes in the distribution of curvature or highlight lines are not wanted because they distort reflections and make the product appear less well designed. When the surfaces generated from the obstacle course quad-meshes (see Fig. 3(b)) avoid artifacts, the construction will be deemed *geometry-suitable*. The automotive design industry also uses the term 'Class A surface' [104] to describe spline surfaces with aesthetic, non-oscillating highlight lines. Class A surfaces satisfy, depending on the application area and contractual agreement, certain hard geometric constraints [2]. Remarkably, they allow a mismatch of normals across curves between two surface pieces up to one tenth of a degree, justifying the surface category $C^{1-\epsilon}$ in Fig. 3(a).

2.2 The isogeometric approach

Higher orders of continuity of the solution space are required for correctly solving higher-order differential equations such as the biharmonic equation, Kirchhoff-Love shell formulations [9, 8, 58], the Cahn-Hilliard phase-field model [23] or simplified Navier-Stokes-Korteweg equations. C^1-continuous finite element spaces are needed even when these problems are expressed in the weak formulation [103], e.g. via Galerkin's discretization for solving a partial differential equation [102, 75]. Where the partitions deviate from regular lattices, classical finite elements join typically only C^0. Ignoring the required differentiability between elements and computing piecemeal in the larger C^0 space can give rise to extraneous solutions that do not correspond to physical solutions. For other classes of differential equations, smoothness, while not formally necessary, has been found to improve accuracy, stability or convergence (see e.g. for contact problems [68, 97]).

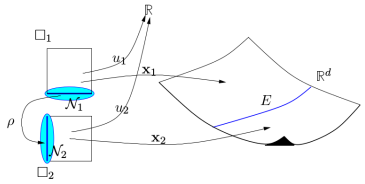

Fig. 5. Atlas $\mathbf{x}$ and analysis functions u_α in the formulation of the fundamental theorem: elements on manifolds $b_i(\mathbf{x}_\alpha) := u_\alpha \circ \mathbf{x}_\alpha^{-1}$ built with geometric continuity across an interface E with the corresponding edges of the domains $\square_1$ and $\square_2$ related by the change of variable ρ.

For a grid-like layout of quadrilateral surface pieces, the practice of using bi-variate splines both for modeling the geometry of the domain and for computing functions on this domain goes back at least to the 1980s [13]. To emphasize the use of B-splines for both geometry and engineering analysis, the term iso-geometric analysis (IGA) was coined in the 2005 publication [29]. Publications that developed the isogeometric approach in the 1980s and 1990s used the less specific and less memorable terms 'higher-order', 'isoparametric' or 'finite elements using NURBS' [93, 3, 4, 91].

A fundamental theorem, [26], asserts that generalized splines whose irregular layout captures free-form shape of surfaces, e.g. G-splines, can directly serve to define isogeometric finite elements. The composition of maps (where $\mathbf{x}_\alpha^{-1}$ is the pull back of $\mathbf{x}_\alpha$) that define the finite elements is illustrated in Fig. 5. G-spline implementations in [72, 35, 73, 74, 89] have confirmed this fact by solving problems of the classical 'finite element obstacle course' [7].

2.3 Requirements for analysis: flexibility-increasing refinability

Examples of functions on surfaces are textures in graphics and deformation stress in engineering analysis. Both may need to have increased resolution, even when the surface

remains the same. [16] shows that C^2-connected bi-cubics have a sub-optimal approximation order in the presence of extraordinary points and, more generally, that refinement of the domain (h-refinement) in the presence of non-trivial reparameterizations fuses the refined polynomial surface pieces of degree p when the continuity is C^{p-1}. Similarly, in the context of geometric modeling, [79] proved that for bi-3 (bicubic) spline patches the interdependence of partial derivatives forces a minimum separation of the extraordinary points when polynomial pieces are joined G^1 or else they fuse. ([16] uses the term 'locking' for the artificial algebraic stiffness; while evocative this term already has a fixed meaning in the thin-shell community). An alternative term for flexibility-increasing refinability is *analysis-suitability*, hence the title of this paper.

To formalize flexibility-increasing refinability, we follow the exposition of [55] and define smoothness between non-overlapping pieces of manifolds as follows.

Definition 1 (G^κ constraints). *Two regular and sufficiently smooth surface pieces $\tilde{\mathbf{f}}, \mathbf{f} : (u,v) \in \mathbb{R}^2 \to \mathbb{R}^d$ that share a boundary curve $\mathbf{e}$* join *G^κ* along *$\mathbf{e}$ if there exists a suitably oriented and non-singular reparameterization $\rho : \mathbb{R}^2 \to \mathbb{R}^2$ so that the partial derivatives $\partial^k \tilde{\mathbf{f}}$ and $\partial^k(\mathbf{f} \circ \rho)$, $k = 0, 1, \ldots, \kappa$, agree along $\mathbf{e}$.*

Let, according to the focus of this survey, the surface pieces be sufficiently smooth piecewise polynomials, e.g. tensor-product splines, and fix the reparameterization $\rho_{\mathbf{e}}$ for every edge $\mathbf{e}$. Then the splines joined with these reparameterizations form a space G_ρ linear in the unconstrained polynomial coefficients. That is, any linear combination of elements in G_ρ associated with these free coefficients (set to 1 and all others to 0) is again in G_ρ.

The space G_ρ is (binarily) *refinable* to a space $\dot{G}_{\dot\rho}$ in the following sense, see Fig. 6. For each piece $\mathbf{f} \in G_\rho$ restricted to $\square := [0..1]^2$, the space $\dot{G}_{\dot\rho}$ has four polynomial pieces $\mathbf{f}^r$, $r = 1, 2, 3, 4$ (wlog. of the same degree as $\mathbf{f}$) defined on the four quarters of $\square$ and joined by the following reparameterizations $\dot\rho$:

$$\dot\rho_{\mathbf{e}^0}(u,v) = \rho_{\mathbf{e}}(\frac{u}{2}, \frac{v}{2}), \quad \dot\rho_{\mathbf{e}^1}(u,v) = \rho_{\mathbf{e}}(\frac{1}{2} + \frac{u}{2}, \frac{v}{2}).$$

Then there is a choice of $\mathbf{f}^r$, namely applying de Casteljau's algorithm to $\mathbf{f}$ at $u = v = 1/2$, so that any element $\mathbf{f} \in G_\rho$ can be represented in $\dot{G}_{\dot\rho}$. That is, $\dot{G}_{\dot\rho}$ refines G_ρ. However, $\dot{G}_{\dot\rho}$ is a larger space than G_ρ since many other choices of macro-patches $\mathbf{f}^r$ are allowable. $\dot{G}_{\dot\rho}$ can therefore be expected to provide more flexibility than G_ρ. The additional degrees of freedom are new coefficients not constrained by enforcing smoothness.

Definition 2 (flexibility-increasing refinable). *A construction is* flexibility-increasing refinable *if, for each domain piece $\square$, $\dot{G}_{\dot\rho} \supsetneq G_\rho$ has more degrees of freedom than G_ρ, both along map boundaries and in the interior.*

Since all new internal transitions arising from refinement must be parametrically C^2 to reproduce the original polynomial pieces by the finer construction, macro-patches are internally C^k rather than G^k, see the black transitions in Fig. 6 are C^k. Having covered the requirements, we now survey in more detail the three ingredients of hybrid constructions: subdivision, G-spline and guide surfaces.

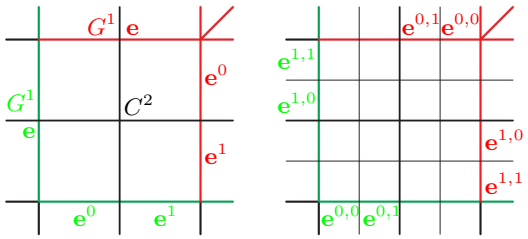

(a) initial (b) refined

Fig. 6. Illustrating flexibility-increasing refinement of a macro-patch. To be flexibility-increasing, new degrees of freedom must appear both in the interior and along the red sector-separating curve boundaries and the darkgreen boundaries that connect the cap to the remaining surface. Second superscripts in (b) enumerate the (second) splitting of the original edges into parts 0 and 1.

3 Subdivision surfaces

More than 40 years ago Catmull and Clark [14] suggested a simple way to smoothly approximate quad meshes by an infinite sequence of nested rings of bi-3 splines; and Doo and Sabin [19] independently generalized bi-2 splines while deriving important mathematical machinery to analyze the resulting surfaces. Following the landmark papers [18, 96] that demonstrated industry support, Catmull-Clark surfaces are nowadays the tool of choice for computer animation. More recently, an efficient set of open source libraries for subdivision on massively parallel CPU and GPU architectures has been agreed upon by Pixar and Microsoft [83] and used by Pixar's proprietary animation system.

Closer mathematical analysis shows that Catmull-Clark surfaces have systemic shape deficiencies that preclude their use in high-end modeling for manufacturing [56, 49]: limits of convex meshes become hyperbolic surfaces, transitions at T-junctions are unduly flat and saddle-like configurations result in undesirable pinched highlight lines. Indeed, distortion of highlight lines for higher valences is a challenge for two members of the category 'singular' in Fig. 3(a): subdivision surfaces and singular jet surfaces. (Only polar surfaces, where one edge is collapsed into a pole, thrive on high valence. Subdivision surfaces can be thought of as collapsing patch size and singular jet surfaces as collapsing the Taylor expansion at a vertex[77, 84, 85, 74, 98]) Indeed, the monograph on the mathematics of subdivision surfaces characterizes subdivision surfaces near irregularities as spline surfaces with singularities [82].

Optimizations of parameters and prescription of the expansion at the extraordinary central point [34, 5, 61, 69] have improved shape outcomes by making the subdivision matrix less sparse. (The subdivision matrix maps control nets surrounding an irregular node to a contracted control net, each of which defines a surface ring, see Fig. 7.) Guided subdivision [38, 50] stabilizes the shape at the cost of a yet denser subdivision matrix. This enables accelerated contraction towards the extraordinary point without noticeable harm to the shape [48]. For example, one high speed contraction step can shrink the remaining hole by more than two steps of Catmull-Clark subdivision as illustrated in Fig. 11. Accelerated, guided subdivision is a key ingredient of hybrid constructions.

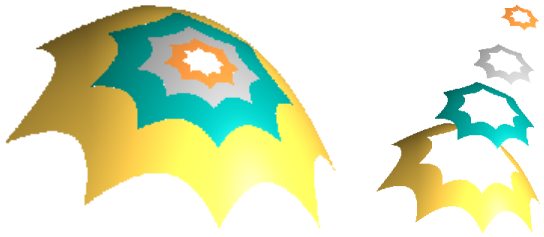

Fig. 7. (*left*) Subdivision surface (from [38]) built from (*right*) a sequence of contracting surface rings.

4 G-splines

While early publications [10, 87, 30, 17, 62, 11, 21] hint at the potential of polynomial pieces joined by a change of variables to fill multi-sided holes in a spline complex, it is arguably Hahn's use of geometric continuity [27] that set the standard for the first generation of G-spline constructions in the 1990s. The focus of the early constructions was on varying the parameterization ρ of Eq. (1) to allow different relations between patch derivatives at irregular non-4-valent points versus regular ones. Expansion by the chain rule of differentiation yields for example G^1 and G^2 constraints in terms of univariate scalar maps $a, b, d, e : u \in \mathbb{R} \to \mathbb{R}$ (partial derivatives of the two coordinates of ρ evaluated on the edge parameterized by $(u, 0)$) and the vector-valued functions $\mathbf{f}$, $\tilde{\mathbf{f}}$ evaluated at $(u, 0)$:

$$\partial_v \tilde{\mathbf{f}} = a\, \partial_v \mathbf{f} + b\, \partial_u \mathbf{f}, \tag{1}$$

$$\partial^2_{vv} \tilde{\mathbf{f}} = a^2\, \partial^2_{vv} \mathbf{f} + 2a\, b\, \partial_u \partial_v \mathbf{f} + b^2\, \partial^2_{uu} \mathbf{f} + d\, \partial_v \mathbf{f} + e\, \partial_u \mathbf{f}. \tag{2}$$

Since neither $\mathbf{f}$ (the rules for constructing the polynomial pieces) nor ρ (the reparameterization) are known a priori, the constraints define a large non-linear space to explore. Considering ρ free to choose increases the space of possible construction. However all sufficiently smooth constructions have to obey a constraint that arises from the circular arrangement of patches surrounding a point, the vertex enclosure constraint [76]. Moreover, the degree of ρ is bounded by the degree of the surface pieces [76] due to what is now understood to be a syzygy relation, see e.g. [70]. Moreover, to create a manifold, the composition of n copies of ρ (across each of the sector-separating curves around an interior point) has to form the identity map, up to the degree of smoothness [78].

Choosing ρ to Hermite interpolate and so separate the computation at either end of an edge between two patches, simplifies solving the system of equations in the polynomial coefficients of Eqs. (1) and (2) but results in many unconstrained coefficients: Hahn and Gregory's early G^2 construction used pieces of degree 18 in u and in v (bi-18) [24] and [106, 57] of degree bi-9. Modern G-splines include G^2 constructions of degree as low as bi-5. Throughout the 1990s work focused on optimizing ρ to minimize the polynomial degree of the surface. Although compatible with the NURBS standard adopted by the manufacturing industries, the shape of early G-spline constructions was often worse than that of subdivision surfaces.

The first decade of this millennium saw improved shape, e.g. [63, 66] still of degree bi-7. Also the distinction between smoothness in the large, assessed via highlight lines, and infinitesimal smoothness, measured as matching derivatives came into focus: a formally only G^1 construction of degree bi-5 or bi-4 [42, 49] showed better curvature distribution than higher degree curvature continuous constructions; and, remarkably, $C^{1-\epsilon}$ construction in [41] trades a slight mismatch in the normal (still within the bounds of class A surfaces) for good highlight line distributions over the multi-sided patch constructed from a finite number of bi-3 patches; the quality of the highlight line distributions could not be matched by the subdivision surfaces of the time (except of the guided variety, see e.g. [47] and Section 5). Additionally, the degree of formally G^2 surfaces with a single patch per sector was reduced to bi-6 [44]. and to degree bi-5 for 2×2 macro-patches [40]. Special scaffold- and sphere-like configurations even allow for curvature continuous bi-4 constructions [43].

A next step forward for G-splines was to allow not only irregular points but also T-junctions as part of a generalized B-spline control net for free-form modeling [36]. T-junctions occur where two quads on one side meet one facet on the other and serve in polyhedral modeling to start or stop quad-strips and so increase or decrease the number of free points to be set. T-junctions prominently feature in quad-dominant remeshing (see e.g. [1, 60, 31, 90]) where they allow to side-step the otherwise stringent global quad-meshing constraints (see e.g. [32, 12, 71]). Also popular in this context are (isolated) triangles that merge and so reduce the number of quad-strips, see Fig. 8. The novelty is that all mesh nodes act as coefficients of linear combinations of piecewise polynomials, i.e. as B-spline-like control points.

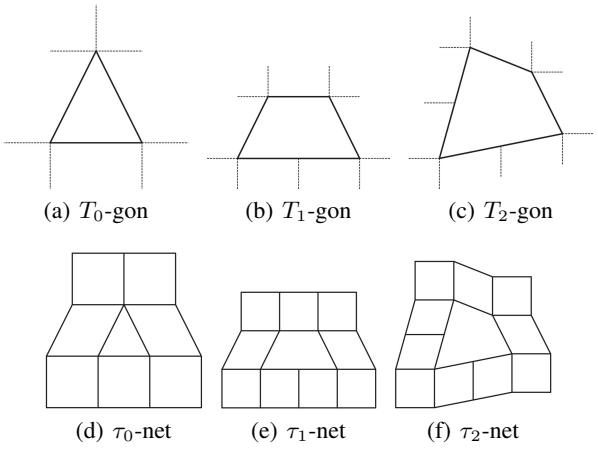

Fig. 8. T-gons and τ-configurations. The subscript counts the number of T-junctions.

While G-splines for multi-sided holes or generalized subdivision can, in principle, convert quad-dominant meshes with T-junctions into smooth surfaces, they do not preserve the two preferred directions and so cause visible shape artifacts. Hierarchical

and T-splines such as [59, 92, 22] need to carefully coordinate knot intervals to admit meshes with T-gons as control nets. For many meshes a globally consistent choice of intervals is impossible [36]. That is, these approaches excel at refining tensor-product patches, but may not be able to produce a smooth surface from a given polyhedral mesh including T-junctions.

The G^1 constructions [51, 53, 52] differ in their polynomial degree, their flexibility-increasing refinability and how close their τ-nets can be placed to each other and to irregular nodes. Built from pieces of degree 3×5, [51] is suitable for modeling class A surfaces. And by complementing the existing G-spline constructions for multi-sided facets, splines for the τ-configurations of Fig. 8 allow interpreting locally quad-dominant meshes as spline control nets.

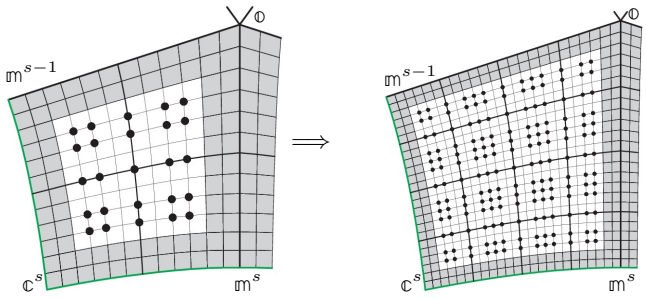

(a) initial 2×2 bi-6 G^2 (b) once-refined bi-6 G^2

Fig. 9. Internal degrees of freedom of refinement of [55] marked as $\bullet$.

Since the majority of high-end surface constructions now are G-splines, their flexibility-increasing refinability has come under scrutiny. The detailed analysis of flexibility-increasing-refinement of [42] showed that, unlike for tensor-product splines, the resulting unconstrained new coefficients (degrees of freedom) are not convenient geometric handles due to their irregular distribution and support [45]. Indeed the full characterization of G^2 flexibility-increasing refinability in [55] proves that multi-sided refinement of G-splines can not be flexibility-increasing when the construction uses bi-5 macro-patches, regardless of the number of $N \times N$ pieces. Conversely, [55] exhibits a bi-6 construction with 2×2 pieces per sector that is G^2 flexibility-increasing refinable, see Fig. 9. (A bi-4 publication, currently under review, presents parallel results for the construction of multi-sided G^1 surfaces.)

5 Guided surfaces

Guided Subdivision [38] is an effective tool to overcome the defects of standard subdivision algorithms. Moreover, unlike standard subdivision, guided subdivision can easily define curvature continuous subdivision surfaces with controllable polynomial reproduction at the limit point. Fig. 10 illustrates the underlying principle: the control mesh

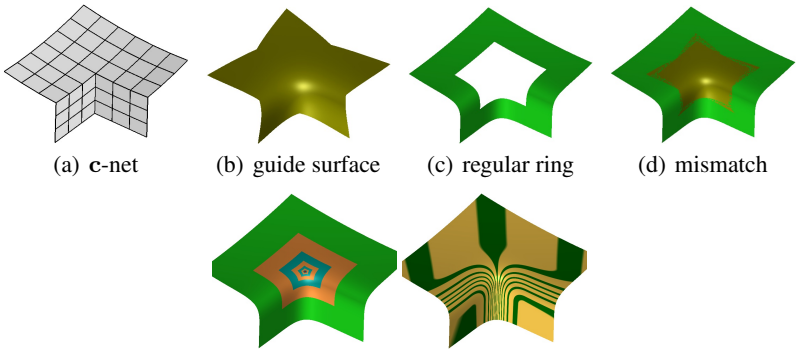

(a) **c**-net (b) guide surface (c) regular ring (d) mismatch

(e) guided rings

Fig. 10. Guided Subdivision. At each step, the preceding ring provides a Hermite prolongation to set the outer coefficients of the next, nested ring while sampling the guide shape yields the inner coefficients.

(a) defines a guide surface (b) and the Hermite prolongation of the surrounding regular ring (c). Since the guide surface and the surrounding surface frame do not fit together as illustrated in (d), the subdivision step retains the outer part of the ring that fits its predecessor ring and determines its new inner part by sampling the guide. The result is shown in (e). We note that the guide surface can have a different structure, smoothness and polynomial degree than the final surface. For example, it can consist of 3-sided patches, whereas the final surface consists of 4-sided patches. Remarkably the overall process is linear and stationary and can so be interpreted as subdivision with large stencil, i.e. with a denser subdivision matrix than Catmull-Clark subdivision. While the rules become more complex, the mathematical analysis of the limit becomes much simpler – and the shape is far better [49].

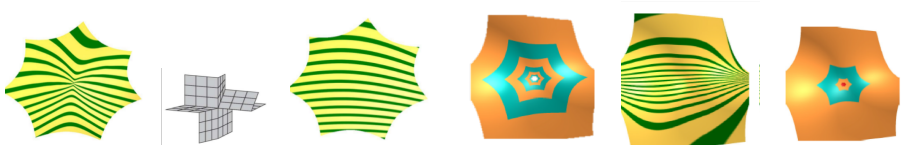

(a) CC (b) $n = 7$ (c) Guided (d) 6 rings (e) shared (f) 3 rings

Fig. 11. Guided Subdivision and Accelerated Guided Subdivision. The highlight line distributions for input **c**-net (b) for (a) Catmull Clark subdivision and (c) Guided Subdivision. For a different input $n = 6$, surfaces (d) and (f) have visually the same highlight line distribution shown in (e).

Moreover, since guided subdivision stabilizes the shape, an additional technique can be leveraged: *accelerated* guided subdivision [81, Sect 5], [48] widens the surface rings and so achieves a more rapid contraction of the remaining gap, see Fig. 11. When the surface rings and final cap follow a guiding shape, good highlight line distributions are

obtained for the shape obstacle course Fig. 3(a), already when the accelerated sequence of C^k-joined surface rings is G^1 completed after 2 or 3 rings, see Fig. 11d, e.

We note that guides can equally well be applied to finite constructions in order to harness excess free parameters. In hybrid surfaces, the same guide surface is applied both to accelerated subdivision rings and the final tiny cap.

6 Hybrid surfaces

While guided subdivision improves shape, it does not address the problem of infinite recursion. Stopping the recursion after a few steps and filling the remaining hole with a triangulated multi-sided facet leads to noticeable flaws in the highlight line rendering. A better solution is to fit a multi-sided G^1-cap. Since the resulting surface consists of a fixed number of surface pieces, it is industry compatible. To combine the best features of subdivision and geometrically continuous surface constructions, we observe that in practice, design and analysis can often predict a maximal level of refinement. When the maximal anticipated refinement level at the irregularity suffices, the cap need not be refined and refinement in the surrounding finite coarser surface requires only standard spline knot insertion [46]. If the anticipated level does not suffice, it is easy to reconstruct with additional surface rings – or once can use a more complex geometrically smooth flexibility-increasing-refinable construction such as Fig. 9.

The earliest hybrid construction, [41], addressed whether bi-cubic surfaces can be class A. The construction, of a main body and cap of degree bi-3, is formally only C^0, with empirically less than a 0.1° normal mismatch between the surrounding surface and the main body. The default uses just three pieces per L-shape and one piece for the limit. The results, summarized visually in [41, Fig. 1] show the hybrid to noticeably improve on methods that yield a formally smoother result [14, 25, 67]. The focus of [47] is on improving the shape of subdivision surfaces by constructing both a C^2 subdivision algorithm generating surfaces of polynomial degree bi-6. An appendix adds G^1 parameterized tiny cap. The full concept of a hybrid construction, including acceleration to obtain few pieces, is realized in [46] (see Fig. 1). In [48] the degree of the C^2 main body is reduced to bi-5. In [49], see Fig. 2, the degree is bi-4 using macro-patches. The approaches use guide surfaces built from n three-sided patches with high smoothness at the central point. Finally [55] proves that the central caps of [46, 48, 49] are not flexibility-increasing refinable and presents a bi-6 tiny cap that both completes the surface G^2 to be is flexibility-increasing refinable. For practical purposes the latter may be more than needed: G^1 suffices up to fourth order differential operators and good geometric shape can be guaranteed by tiny G^1 caps whose refinement is much simpler, pointing to [48] as the method of choice.

The key ingredient of hybrid constructions is the guide surface and the sampling, via characteristic maps Fig. 12, of Hermite data along the sequences of boundary curves of the patches. Presented in BB-form these Hermite data are called tensor-borders. For details on the characteristic maps see [48]. The rapid contraction of the guided rings means that the resulting macro-patches consist of few pieces per sector, e.g. of seven pieces: three for each of two polynomial L-shapes and one for the central G-spline patch. This yields smooth surfaces consisting of a finite number of pieces whose for-

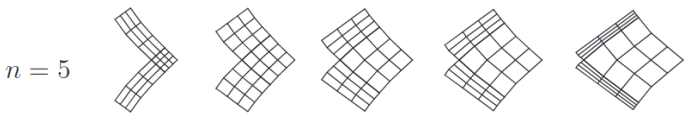

Fig. 12. A sector of the characteristic map for $n = 5$ and speeds $\frac{1}{4}, \frac{1}{2}, \frac{2}{3}, \frac{3}{4}, \frac{7}{8}$ from [39].

mulas derive linearly from the input control net, hence can be implemented, for fixed contraction speed and valence, as a single matrix multiplication applied to the local control net. In practice, for [48], one splits the matrix into a 21×31 matrix for creating a sector of the guide, a 21×21 matrix for the de Casteljau steps that re-represent the guide for a contracted domain, a 27×21 matrix defining one sector of the prolongation of the L-shape and 36×21 matrix for one sector of the tiny cap.

7 Conclusion

In order to advertise a useful class of piecewise polynomial surface constructions for filling multi-sided holes in a smooth spline complex, we surveyed subdivision, G-spline and guided surfaces. Combining accelerated guided subdivision with a tiny G-spline cap yields a number of advantages for modelling and analysis: good shape, easy implementation and simple refinability up to a pre-defined level.

References

1. Pierre Alliez, David Cohen-Steiner, Olivier Devillers, Bruno Lévy, and Mathieu Desbrun. Anisotropic polygonal remeshing. In Jessica Hodgins and John C. Hart, editors, *Proceedings of ACM SIGGRAPH 2003*, volume 22(3) of *ACM Transactions on Graphics*, pages 485–493. ACM Press, 2003.
2. Zoran Andjelic. What is the definition of a class A surface?, accessed May 2015. https://grabcad.com/questions/what-is-definition-of-class-a-surface.
3. Francis T.K. Au and Y.K. Cheung. Spline finite elements for beam and plate. *Computers & Structures*, 37:717–729, 1990.
4. Francis T.K. Au and Y.K. Cheung. Isoparametric spline finite strip for plane structures. *Computers & Structures*, 48:22–32, 1993.
5. Ursula H. Augsdoerfer, Neil A. Dodgson, and Malcolm A. Sabin. Removing polar rendering artifacts in subdivision surfaces. *J. Graphics, GPU, & Game Tools*, 14(2):61–76, 2009.
6. Klaus-Peter Beier and Yifan Chen. Highlight-line algorithm for realtime surface-quality assessment. *Computer-Aided Design*, 26(4):268–277, 1994.
7. Ted Belytschko, Henryk Stolarski, Wing Kam Liu, Nicholas Carpenter, and Jame SJ Ong. Stress projection for membrane and shear locking in shell finite elements. *Computer Methods in Applied Mechanics and Engineering*, 51(1):221–258, 1985.
8. D. J. Benson, Y. Bazilevs, M.-C. Hsu, and T. J. R. Hughes. A large deformation, rotation-free, isogeometric shell. *Computer Methods in Applied Mechanics and Engineering*, 200(13):1367–1378, 2011.

9. D.J. Benson, S. Hartmann, Y. Bazilevs, M.-C. Hsu, and T.J.R. Hughes. Blended isogeometric shells. *Computer Methods in Applied Mechanics and Engineering*, 255:133–146, 2013.
10. Pierre E. Bezier. *Essai de definition numerique des courbes et des surfaces experimentales*. Ph.d. thesis, Universite Pierre et Marie Curie, February 1977.
11. W. Boehm. Smooth curves and surfaces. In G. Farin, editor, *Geometric Modeling: Algorithms and New Trends*, pages 175–184. SIAM, Philadelphia, 1987.
12. David Bommes, Marcel Campen, Hans-Christian Ebke, Pierre Alliez, and Leif Kobbelt. Integer-grid maps for reliable quad meshing. *ACM Trans. Graph*, 32(4):98:1–98:12, 2013.
13. V. Braibant and C. Fleury. Shape optimal design using B-splines. *CMAME*, 44:247–267, 1984.
14. E. Catmull and J. Clark. Recursively generated B-spline surfaces on arbitrary topological meshes. *Computer-Aided Design*, 10:350–355, September 1978.
15. P. Charrot and J. Gregory. A pentagonal surface patch for computer aided geometric design. *Computer Aided Geometric Design*, 1(1), 1984.
16. Annabelle Collin, Giancarlo Sangalli, and Thomas Takacs. Analysis-suitable G^1 multi-patch parametrizations for C^1 isogeometric spaces. *Computer Aided Geometric Design*, 47:93–113, 2016.
17. T. DeRose. *Geometric Continuity: A Parametrization Independent Measure of Continuity for Computer Aided Design*. PhD thesis, UC Berkeley, California, 1985.
18. Tony DeRose, Michael Kass, and Tien Truong. Subdivision surfaces in character animation. In *Proceedings of the ACM Conference on Computer Graphics (SIGGRAPH-98)*, pages 85–94, New York, July 19–24 1998. ACM Press.
19. D. Doo and M. Sabin. Behaviour of recursive division surfaces near extraordinary points. *Computer-Aided Design*, 10:356–360, September 1978.
20. G. Farin. *Curves and Surfaces for Computer Aided Geometric Design: A Practical Guide*. Academic Press, 1988.
21. T. Garrity and J. Warren. Geometric continuity. *Computer Aided Geometric Design*, 8(1):51–66, February 1991.
22. Carlotta Giannelli, Bert Jüttler, and Hendrik Speleers. THB-splines: The truncated basis for hierarchical splines. *Computer Aided Geometric Design*, 29(7):485–498, 2012.
23. H. Gomez, V. M Calo, Y. Bazilevs, and T. J. R. Hughes. Isogeometric analysis of the Cahn–Hilliard phase-field model. *CMAME*, 197(49):4333–4352, 2008.
24. John A. Gregory and Jorg M. Hahn. A C^2 polygonal surface patch. *Comp Aided Geom Design*, 6(1):69–75, 1989.
25. John A. Gregory and Jianwei Zhou. Filling polygonal holes with bicubic patches. *Computer Aided Geometric Design*, 11(4):391–410, 1994.
26. David Groisser and Jörg Peters. Matched G^k-constructions always yield C^k-continuous isogeometric elements. *Computer Aided Geometric Design*, 34:67–72, March 2015. PMC4432484.
27. Jorg M. Hahn. Geometric continuous patch complexes. *Computer Aided Geometric Design*, 6(1):55–67, 1989.
28. Gerben J. Hettinga and Jiri Kosinka. Phong Tessellation and PN Polygons for Polygonal Models. In Adrien Peytavie and Carles Bosch, editors, *EG 2017 - Short Papers*. The Eurographics Association, 2017.
29. T. J. R. Hughes, J. A. Cottrell, and Y. Bazilevs. Isogeometric analysis: CAD, finite elements, NURBS, exact geometry and mesh refinement. *Computer Methods in Applied Mechanics and Engineering*, 194:4135–4195, 2005.
30. Kahmann J. *Continuity of curvature between adjacent Bézier patches*, pages 65–75. North-Holland Publishing Company, Amsterdam, 1983.

31. Wenzel Jakob, Marco Tarini, Daniele Panozzo, and Olga Sorkine-Hornung. Instant field-aligned meshes. *ACM Trans. Graph*, 34(6):189, 2015.
32. Felix Kälberer, Matthias Nieser, and Konrad Polthier. Quadcover - surface parameterization using branched coverings. *Comput. Graph. Forum*, 26(3), 2007.
33. Mario Kapl, Vito Vitrih, Bert Jüttler, and Katharina Birner. Isogeometric analysis with geometrically continuous functions on two-patch geometries. *Computers & Mathematics with Applications*, 70(7):1518–1538, 2015.
34. Kęstutis Karčiauskas, Ashish Myles, and Jörg Peters. A C^2 polar jet subdivision. In A. Scheffer and K. Polthier, editors, *Proceedings of Symposium of Graphics Processing (SGP), June 26-28 2006, Cagliari, Italy*, pages 173–180. ACM Press, 2006.
35. Kęstutis Karčiauskas, Thien Nguyen, and Jörg Peters. Generalizing bicubic splines for modelling and IGA with irregular layout. *Computer Aided Design*, 70:23–35, Jan 2016.
36. Kęstutis Karčiauskas, Daniele Panozzo, and Jörg Peters. T-junctions in spline surfaces. *ACM Tr on Graphics, ACM Siggraph*, 36(5):170:1–9, 2017.
37. Kęstutis Karčiauskas and Jörg Peters. Quad-net obstacle course. http://www.cise.ufl.edu/research/SurfLab/shape_gallery.shtml. Accessed: June 2020.
38. Kęstutis Karčiauskas and Jörg Peters. Concentric tesselation maps and curvature continuous guided surfaces. *Computer-Aided Geometric Design*, 24(2):99–111, Feb 2007.
39. Kęstutis Karčiauskas and Jörg Peters. Adjustable speed surface subdivision. *Computer Aided Geometric Design.*, 26:962–969, 2009.
40. Kęstutis Karčiauskas and Jörg Peters. Biquintic G^2 surfaces via functionals. *Computer Aided Geometric Design*, pages 17–29, 2015.
41. Kęstutis Karčiauskas and Jörg Peters. Can bi-cubic surfaces be class A? *Computer Graphics Forum*, 34(5):229–238, August 2015.
42. Kęstutis Karčiauskas and Jörg Peters. Improved shape for multi-surface blends. *Graphical Models*, 8:87–98, 2 2015.
43. Kęstutis Karčiauskas and Jörg Peters. Curvature continuous bi-4 constructions for scaffold- and sphere-like surfaces. *Computer Aided Design (SPM 2016)*, 78:48–59, June 17 2016.
44. Kęstutis Karčiauskas and Jörg Peters. Minimal bi-6 G^2 completion of bicubic spline surfaces. *Computer Aided Geometric Design*, 41:10–22, Jan 2016.
45. Kęstutis Karčiauskas and Jörg Peters. Refinable G^1 functions on G^1 free-form surfaces. *Computer Aided Geometric Design*, 54:61–73, May 2017.
46. Kęstutis Karčiauskas and Jörg Peters. Fair free-form surfaces that are almost everywhere parametrically C^2. *Journal of Computational and Applied Mathematics*, pages 1–10, 2018. PMC6474374.
47. Kęstutis Karčiauskas and Jörg Peters. A new class of guided C^2 subdivision surfaces combining good shape with nested refinement. *Computer Graphics Forum*, 37:84–95, 2018.
48. Kęstutis Karčiauskas and Jörg Peters. Rapidly contracting subdivision yields finite, effectively C^2 surfaces. *Computers & Graphics*, pages 1–10, 2018.
49. Kęstutis Karčiauskas and Jörg Peters. Refinable bi-quartics for design and analysis. *Computer-Aided Design*, pages 1–10, 2018. PMC6474386.
50. Kęstutis Karčiauskas and Jörg Peters. Curvature-bounded guided subdivision: biquartics vs bicubics. *Computer Aided Design*, pages 1–11, Jul 2019.
51. Kęstutis Karčiauskas and Jörg Peters. High quality refinable G-splines for locally quad-dominant meshes with T-gons. *Computer Graphics Forum*, 38(5):151–161, Aug 2019.
52. Kęstutis Karčiauskas and Jörg Peters. Localized G-splines for quad & T-gon meshes. *Computer Aided Geometric Design*, 71:244–254, May 2019. PMC7441736.
53. Kęstutis Karčiauskas and Jörg Peters. Refinable smooth surfaces for locally quad-dominant meshes with T-gons. *Computers & Graphics*, 82:193–202, Aug 2019. PMC7437788.
54. Kęstutis Karčiauskas and Jörg Peters. Low degree splines for locally quad-dominant meshes. *Computer Aided Geometric Design*, 83:1–12, 2020. PMC7561030.

55. Kęstutis Karčiauskas and Jörg Peters. A sharp degree bound on G^2-refinable multi-sided surfaces. *Comput Aided Des.*, to appear:1–12, 2020. PMC7295118.
56. Kęstutis Karciauskas, Jörg Peters, and Ulrich Reif. Shape characterization of subdivision surfaces – case studies. *Computer-Aided Geometric Design*, 21(6):601–614, july 2004.
57. Przemyslaw Kiciak. Spline surfaces of arbitrary topology with continuous curvature and optimized shape. *Computer-Aided Design*, 45(2):154–167, 2013.
58. J. Kiendl, K.-U. Bletzinger, J. Linhard, and R. Wüchner. sogeometric shell analysis with kirchhoff-love elements. *Computer Methods in Applied Mechanics and Engineering*, 198(49):3902–3914, 2009.
59. R. Kraft. *Adaptive und linear unabhängige Multilevel B-Splines und ihre Anwendungen*. PhD thesis, University of Stuttgart, 1998.
60. Yu-Kun Lai, Leif Kobbelt, and Shi-Min Hu. An incremental approach to feature aligned quad dominant remeshing. In Eric Haines and Morgan McGuire, editors, *Symposium on Solid and Physical Modeling*, pages 137–145. ACM, 2008.
61. Xin Li, G.T. Finnigan, and T.W. Sederberg. G^1 non-uniform Catmull-Clark surfaces. *ACM Trans. Graph*, 35(4):135:1–135:8, 2016.
62. Ding-yuan Liu. A geometric condition for smoothness between adjacent bézier surface patches. *Acta Mathematicae Applicatae Sinica*, 9(4), 1986.
63. Charles Loop. Second order smoothness over extraordinary vertices. In *Symp Geom Processing*, pages 169–178, 2004.
64. Charles Loop and Scott Schaefer. Approximating Catmull–Clark subdivision surfaces with bicubic patches. *ACM Transactions on Graphics*, 27(1):8:1–8:11, March 2008.
65. Charles T. Loop and Tony D. DeRose. A multisided generalization of Bézier surfaces. *ACM Trans. Graph.*, 8(3):204–234, July 1989.
66. Charles T. Loop and Scott Schaefer. G^2 tensor product splines over extraordinary vertices. *Comput. Graph. Forum*, 27(5):1373–1382, 2008.
67. Charles T. Loop, Scott Schaefer, Tianyun Ni, and Ignacio Castaño. Approximating subdivision surfaces with Gregory patches for hardware tessellation. *ACM Trans. Graph*, 28(5), 2009.
68. L De Lorenzis, I Temizer, P Wriggers, and G Zavarise. A large deformation frictional contact formulation using NURBS-based isogeometric analysis. *International Journal for Numerical Methods in Engineering*, 87(13):1278–1300, 2011.
69. Yue Ma and Weiyin Ma. Subdivision schemes with optimal bounded curvature near extraordinary vertices. *Comput. Graph. Forum*, 37(7):455–467, 2018.
70. Bernard Mourrain, Raimundas Vidunas, and Nelly Villamizar. Geometrically continuous splines for surfaces of arbitrary topology. *Computer Aided Geometric Design*, 45:108–133, July 2016.
71. Ashish Myles, Nico Pietroni, and Denis Zorin. Robust field-aligned global parametrization. *ACM Trans. Graph.*, 33(4):135:1–135:14, July 2014.
72. Thien Nguyen, Kęstutis Karčiauskas, and Jörg Peters. A comparative study of several classical, discrete differential and isogeometric methods for solving Poisson's equation on the disk. *Axioms*, 3(2):280–299, Jan 2014.
73. Thien Nguyen, Kęstutis Karčiauskas, and Jörg Peters. C^1 finite elements on non-tensor-product 2d and 3d manifolds. *Applied Mathematics and Computation*, 272(1):148–158, 2016. PMC4652325.
74. Thien Nguyen and Jörg Peters. Refinable C^1 spline elements for irregular quad layout. *Computer Aided Geometric Design*, 43:123–130, March 29 2016. PMC4834718.
75. Encyclopedia of Mathematics. Galerkin method, accessed Dec 2020. https://encyclopediaofmath.org/wiki/Galerkin_method.
76. J. Peters. *Fitting smooth parametric surfaces to 3D data*. PhD thesis, University of Wisconsin, 1990. PhD thesis; see also CMS Technical Report 91-2.

77. J. Peters. Parametrizing singularly to enclose vertices by a smooth parametric surface. In S. MacKay and E. M. Kidd, editors, *Graphics Interface '91, Calgary, Alberta, 3–7 June 1991: proceedings*, pages 1–7, 243 College St, 5th Floor, Toronto, Ontario M5T 2Y1, Canada, 1991. Canadian Information Processing Society.
78. J. Peters. A characterization of connecting maps as roots of the identity. *Curves and Surfaces in Geometric Design*, pages 369–376, 1994.
79. J. Peters and Jianhua Fan. On the complexity of smooth spline surfaces from quad meshes. *Computer-Aided Geometric Design*, 27:96–105, 2009.
80. Jörg Peters. Splines for meshes with irregularities. *The SMAI journal of computational mathematics*, S5:161–183, 2019.
81. Jörg Peters and K. Karčiauskas. An introduction to guided and polar surfacing. In *Mathematical Methods for Curves and Surfaces*, volume 5862/2010, pages 299–315. Springer, 2010. Seventh International Conference on Mathematical Methods for Curves and Surfaces Toensberg, Norway, Toensberg, Norway, June 26-July 1, 2008, Revised Selected Papers.
82. Jörg Peters and Ulrich Reif. *Subdivision Surfaces*, volume 3 of *Geometry and Computing*. Springer-Verlag, New York, 2008.
83. Pixar. http://graphics.pixar.com/opensubdiv/docs/intro.html. accessed June 26 2020.
84. Ulrich Reif. *Neue Aspekte in der Theorie der Freiformflächen beliebiger Topologie*. PhD thesis, Math Inst A, U Stuttgart, 1993.
85. Ulrich Reif. A refinable space of smooth spline surfaces of arbitrary topological genus. *Journal of Approximation Theory*, 90(2):174–199, 1997.
86. M. Sabin. Transfinite surface interpolation. volume VI of *Mathematics of Surfaces*, pages 517–534, Oxford, September 1996. Clarendon Press.
87. Malcolm A. Sabin. *The use of Piecewise Forms for the numerical representation of shape*. PhD thesis, Computer and Automation Institute, 1977.
88. Péter Salvi and Tamás Várady. Multi-sided Bézier surfaces over concave polygonal domains. *Computers & Graphics*, 74:56–65, 2018.
89. Giancarlo Sangalli, Thomas Takacs, and Rafael Vázquez Hernández. Unstructured spline spaces for isogeometric analysis based on spline manifolds. *Comput. Aided Geom. Des*, 47:61–82, 2016.
90. Nico Schertler, Marco Tarini, Wenzel Jakob, Misha Kazhdan, Stefan Gumhold, and Daniele Panozzo. Field-aligned online surface reconstruction. *ACM Trans. Graph*, 36(4):77:1–77:13, 2017.
91. Uwe Schramm and Walter D. Pilkey. The coupling of geometric descriptions and finite elements using NURBS - a study in shape optimization. *Finite elements in Analysis and Design*, 340:11–34, 1993.
92. Thomas W. Sederberg, Jianmin Zheng, Almaz Bakenov, and Ahmad Nasri. T-splines and T-NURCCs. In Jessica Hodgins and John C. Hart, editors, *Proceedings of ACM SIGGRAPH 2003*, volume 22(3) of *ACM Transactions on Graphics*, pages 477–484. ACM Press, 2003.
93. Y.K. Shyy, C. Fleury, and K. Izadpanah. Shape optimal design using higher-order elements. *CMAME*, 71:99–116, 1988.
94. J. Smith and S. Schaefer. Selective degree elevation for multi-sided Bézier patches. *Comput. Graph. Forum*, 34(2):609–615, 2015.
95. Hendrik Speleers, Carla Manni, Francesca Pelosi, and M Lucia Sampoli. Isogeometric analysis with powell–sabin splines for advection–diffusion–reaction problems. *Computer methods in applied mechanics and engineering*, 221:132–148, 2012.
96. Jos Stam. Exact evaluation of Catmull-Clark subdivision surfaces at arbitrary parameter values. pages 395–404, New York, July 19–24 1998. ACM Press.
97. Ilker Temizer, P Wriggers, and T. Hughes. Contact treatment in isogeometric analysis with nurbs. *CMAME*, 200(9):1100–1112, 2011.

98. Deepesh Toshniwal, Hendrik Speleers, and Thomas JR Hughes. Smooth cubic spline spaces on unstructured quadrilateral meshes with particular emphasis on extraordinary points: Geometric design and isogeometric analysis considerations. *Computer Methods in Applied Mechanics and Engineering*, 327:411–458, 2017.
99. Tamás Várady, Alyn P. Rockwood, and Péter Salvi. Transfinite surface interpolation over irregular n-sided domains. *Computer-Aided Design*, 43(11):1330–1340, 2011.
100. Tamás Várady, Péter Salvi, and György Karikó. A multi-sided Bézier patch with a simple control structure. *Comput. Graph. Forum*, 35(2):307–317, 2016.
101. Alex Vlachos, Jorg Peters, Chas Boyd, and Jason L. Mitchell. Curved PN triangles. In *2001, Symposium on Interactive 3D Graphics*, Bi-Annual Conference Series, pages 159–166. ACM Press, 2001.
102. wikipedia. Galerkin method, accessed Dec 2020. https://en.wikipedia.org/wiki/Galerkin_method.
103. wikipedia. Weak formulation, accessed Dec 2020. https://en.wikipedia.org/wiki/Weak_formulation.
104. wikipedia. Class_a_surfaces, accessed June 2020. http://en.wikipedia.org/wiki/Class_A_surfaces.
105. Y. Yamada. *Clay Modeling: Techniques for giving three-dimensional form to idea*. Nissan Design Center, Kaneko Enterprises, 1997.
106. Xiuzi Ye. Curvature continuous interpolation of curve meshes. *Computer Aided Geometric Design*, 14(2):169–190, 1997.